Kelch-like protein 42 is a profibrotic ubiquitin E3 ligase involved in systemic sclerosis

Received for publication, December 3, 2019, and in revised form, February 7, 2020 Published, Papers in Press, February 17, 2020, DOI 10.1074/jbc.AC119.012066

Travis B. Lear[‡§], Karina C. Lockwood[§], Mads Larsen[§], Ferhan Tuncer[§], Jason R. Kennerdell[§], Christina Morse[¶], Eleanor Valenzi[¶], Tracy Tabib[¶], Michael J. Jurczak[‖], Daniel J. Kass[**], John W. Evankovich[§‡‡], Toren Finkel[§ §§], Robert Lafyatis[¶], Yuan Liu[§‡‡1], and Bill B. Chen[§‡‡¶¶2]

From the [‡]Department of Environmental and Occupational Health, Graduate School of Public Health, University of Pittsburgh, Pittsburgh, Pennsylvania 15261, the [§]Aging Institute, [¶]Division of Rheumatology and Clinical Immunology, [‖]Division of Endocrinology and Metabolism, [‡‡]Acute Lung Injury Center of Excellence, Division of Pulmonary, Allergy, and Critical Care Medicine, [§§]Division of Cardiology, and [¶¶]Vascular Medicine Institute, Department of Medicine, School of Medicine, University of Pittsburgh, Pittsburgh, Pennsylvania 15213, and the [**]Dorothy P. and Richard P. Simmons Center for Interstitial Lung Disease, School of Medicine, University of Pittsburgh, Pittsburgh, Pennsylvania 15213

Edited by Alex Toker

Systemic scleroderma (SSc) is an autoimmune disease that affects over 2.5 million people globally. SSc results in dysfunctional connective tissues with excessive profibrotic signaling, affecting skin, cardiovascular, and particularly lung tissue. Over three-quarters of individuals with SSc develop pulmonary fibrosis within 5 years, the main cause of SSc mortality. No approved medicines to manage lung SSc currently exist. Recent research suggests that profibrotic signaling by transforming growth factor β (TGF-β) is directly tied to SSc. Previous studies have also shown that ubiquitin E3 ligases potently control TGF-β signaling through targeted degradation of key regulatory proteins; however, the roles of these ligases in SSc–TGF-β signaling remain unclear. Here we utilized primary SSc patient lung cells for high-throughput screening of TGF-β signaling via high-content imaging of nuclear translocation of the profibrotic transcription factor SMAD family member 2/3 (SMAD2/3). We screened an RNAi library targeting ubiquitin E3 ligases and observed that knockdown of the E3 ligase Kelch-like protein 42 (KLHL42) impairs TGF-β–dependent profibrotic signaling. KLHL42 knockdown reduced fibrotic tissue production and decreased TGF-β–mediated SMAD activation. Using unbiased ubiquitin proteomics, we identified phosphatase 2 regulatory subunit B'ϵ (PPP2R5ϵ) as a KLHL42 substrate. Mechanistic experiments validated ubiquitin-mediated control of PPP2R5ϵ stability through KLHL42. PPP2R5ϵ knockdown exacerbated TGF-β–mediated profibrotic signaling, indicating a role of PPP2R5ϵ in SSc. Our findings indicate that the KLHL42–PPP2R5ϵ axis controls profibrotic signaling in SSc lung fibroblasts. We propose that future studies could investigate whether chemical inhibition of KLHL42 may ameliorate profibrotic signaling in SSc.

Systemic sclerosis (SSc)[3] or scleroderma is an autoimmune rheumatic disease affecting numerous tissue and organ systems and is characterized by hardening and fibrosis of connective tissues. SSc manifests prominently in the skin through skin thickening or increased inflammation; however, the primary cause of mortality is SSc-associated interstitial lung disease (SSc-ILD) (1, 2). Over three-quarters of SSc patients develop lung fibrosis within 5 years of diagnosis, with a subset developing progressive fibrotic disease (3). SSc-ILD is characterized by decreased respiratory function because of excessive hardening and fibrotic scarring because of extracellular matrix deposition in the lung. In combination with an increased inflammatory response, epithelial injury, and cellular fibrotic transition, fibrous production and collagen deposition in the lung interstitium lead to respiratory failure (4, 5). Although new therapeutic agents are under evaluation, current treatment options that target the underlying pathophysiology are limited (6). Profibrotic cellular signaling pathways are associated with pathological remodeling of the lungs, leading to SSc-ILD, particularly that of the transforming growth factor β (TGF-β) pathway (4). Research has shown TGF-β cytokine and downstream signaling to have stark causal effects on SSc disease models (7).

TGF-β signaling proceeds through cellular recognition of the TGF-β cytokine by receptor complexes and activation of mothers against decapentaplegic homolog (SMAD) transcription factors (8). In canonical TGF-β/SMAD signal transduction, receptor-regulated SMAD2/3 protein is phosphorylated, complexed with the co-SMAD protein SMAD4, and shuttled to

This work was supported by the University of Pittsburgh Aging Institute seed fund (to B. B. C. and Y. L.); NIDDK, National Institutes of Health Grant 1R01DK119627 (to Y. L. and M. J. J.); NIAMS, National Institutes of Health Grant 5P50AR060780-08 (to R. L., D. J. K., and B. B. C.); and NHLBI, National Institutes of Health Grants 5F31HL143843 (to T. B. L.), 1K08HL144820 (to J. W. E), 5R01HL142777 (to Y. L.), and 5R35HL139860 and 5R01HL133184 (to B. B. C.). The authors declare that they have no conflicts of interest with the contents of this article. The content is solely the responsibility of the authors and does not necessarily represent the official views of the National Institutes of Health.

[1] To whom correspondence may be addressed: Bridgeside Point 1, 100 Technology Dr., Pittsburgh, PA 15219. Tel.: 412-624-2664; E-mail: liuy13@upmc.edu.

[2] To whom correspondence may be addressed: Bridgeside Point 1, 100 Technology Dr., Pittsburgh, PA 15219. Tel.: 412-624-2664; E-mail: chenb@upmc.edu.

[3] The abbreviations used are: SSc, systemic sclerosis; SSc-ILD, systemic sclerosis–associated interstitial lung disease; TGF, transforming growth factor; TUBE, tandem ubiquitin-binding entities; CHX, cycloheximide; KD, knockdown; SMAD, mothers against decapentaplegic homolog; esiRNA, Endoribonuclease-prepared siRNA.

the nucleus, where profibrotic transcription programs are activated (9). Nuclear localization and activating phosphorylation of SMAD transcription factors are essential for their signaling transduction, as numerous studies have shown inhibition of TGF-β signaling upon SMAD inactivation or nuclear exclusion (10–14). SMAD-dependent TGF-β signaling is tightly regulated through a variety of mechanisms, including posttranslational protein degradation pathways (15, 16).

Protein degradation is an evolutionarily conserved process for regulating cellular protein longevity. Dysfunctional or aberrant protein degradation is at the heart of many diseases, including fibrotic signaling in the lung. The major mechanism governing protein degradation is the ubiquitin proteasome system (17). Briefly, the small protein ubiquitin is conjugated to target substrate proteins through an enzymatic cascade, among which the ubiquitin E3 ligase enzyme class plays an essential role in substrate recognition and completion of the ubiquitination process. Ubiquitination is a crucial mechanism to regulate homeostasis in TGF-β signaling, as E3 ligase–mediated degradation of TGF-β receptors and of SMAD2/3 transcription factors helps to dampen signaling (18, 19). However, ubiquitination is associated with pathologic fibrotic signaling; we and other groups have observed ubiquitination proteins affecting multiple facets of fibrotic signaling in the lung, including the TGF-β pathway (15, 20–23). Further, profibrotic E3 ligases have also shown promise as targets for chemical inhibition to reduce deleterious fibrotic signaling (21, 24–26). To uncover new ubiquitin E3 ligases regulators of SSc fibrotic signaling, we utilized a high-throughput imaging system to screen an RNAi library targeting E3 ligases for their effect on SMAD2/3 translocation in SSc lung fibroblasts.

Here we report the development of SSc lung fibroblasts as a screening tool for TGF-β activation based on SMAD2/3 nuclear translocation. We identified the ubiquitin E3 ligase KLHL42 as a profibrotic mediator of TGF-β–SSc fibrotic signaling. KLHL42 was also shown to be a regulator of the stability of the protein phosphatase 2A regulatory subunit PPP2R5ϵ and may regulate fibrotic signaling through the PP2A pathway. This study provides a new model of E3 ligase control for fibrotic signaling in SSc lung disease.

Results

Development of the SMAD2/3 translocation ratio screening assay

The Systemic Sclerosis Center of Research Translation at the University of Pittsburgh works with the University of Pittsburgh Medical Center for collection of tissue and explant samples from SSc patients for research. Through this center, we utilized primary SSc patient lung fibroblasts in culture as the basis for the high-content screening assay. Previous research has demonstrated that SSc cell cultures have increased TGF-β/SMAD signaling and exhibit a strongly profibrotic phenotype, which would make them ideal for RNAi loss-of-function screening (7, 27, 28).

We first sought to validate SSc cells as a proper tool for high-content screening in a 384-well plate format. Immunofluorescence studies of SSc lung fibroblasts (SSc cells) show responsiveness to TGF-β1 stimulation, leading to an increased SMAD2/3 fluorescence signal in the nucleus (Fig. 1*A*). As a surrogate for overall fibrotic activity, we calculated a translocation ratio metric based on nuclear SMAD2/3 immunostaining relative to cytoplasmic SMAD2/3. As SMAD transcription factors are shuttled to the nucleus for fibrotic signaling, we hypothesized that an increased translocation ratio represented a more fibrotic response. The translocation ratio metric showed robust results through titration of primary and secondary antibodies for both baseline and TGF-β1–stimulated treatments (Fig. 1*B*). We calculated a Z' factor of 0.39 for this assay; this signal window proved to be adequate for screening (Fig. 1*C*) (29). Silencing of an essential protein for the TGF-β/SMAD signaling process would result in a decreased translocation ratio (Fig. 1*D*). We then proceeded to screen for key ubiquitin E3 ligase modulators.

The E3 ligase KLHL42 affects fibrotic signaling and SMAD activation in SSc

With the validation of SSc fibroblasts as a potential screening tool, we sought to screen an Endoribonuclease-prepared siRNA (esiRNA) library (Sigma) against ubiquitination proteins for their effect on SMAD2/3 localization. Following siRNA knockdown and TGF-β1 stimulation, we collected and immunostained SSc fibroblasts for SMAD2/3 protein, conducted automated microscopy, and calculated a translocation ratio for each esiRNA (Fig. 2*A*). We observed that most siRNAs had little effect on the changing translocation ratio relative to control esiRNA, but we observed hits whose silencing reduced the SMAD2/3 translocation ratio (Fig. 2*B*). Given that knockdown of these targets resulted in a reduced translocation ratio (less nuclear SMAD2/3 protein), we hypothesized that these ubiquitination proteins functioned as profibrotic mediators. Of these hits, we observed Kelch-like protein 42 (KLHL42) to be a relatively undercharacterized E3 ligase. Previous studies have suggested that KLHL42 functions as part of the Cullin-3 E3 ligase complex, in which KLHL42 functions as the key substrate-engaging protein to facilitate substrate ubiquitination (30, 31). However, the effect of KLHL42 on fibrotic signaling is unclear. We validated the initial screening data through confocal microscopy, as *KLHL42* knockdown resulted in decreased SMAD2 activation upon TGF-β1. Knockdown of the TGF-βR1 receptor was used as a positive control, as loss of a major membrane receptor for TGF-β1 would impede TGF-β1–mediated activation of SMAD signaling (13) (Fig. 2, *C* and *D*). *KLHL42* knockdown significantly reduced production of fibrotic proteins such as fibronectin (Fig. 2, *E* and *F*). Further, we observed, through an immunoblot assay, that *KLHL42* knockdown affects SMAD2 activation (Ser-465/467 phosphorylation) without changing total SMAD2 protein levels, suggesting that the effect of KLHL42 occurs upstream in the signaling process and not through degradation of the SMAD2 protein (Fig. 2, *G* and *H*). These initial studies suggest that KLHL42 may be a profibrotic E3 ligase.

Unbiased determination of PPP2R5ϵ as a putative KLHL42 substrate

Ubiquitin E3 ligases primarily exert biological function through targeted ubiquitination and degradation of substrate proteins. To uncover the putative KLHL42 substrate, we con-

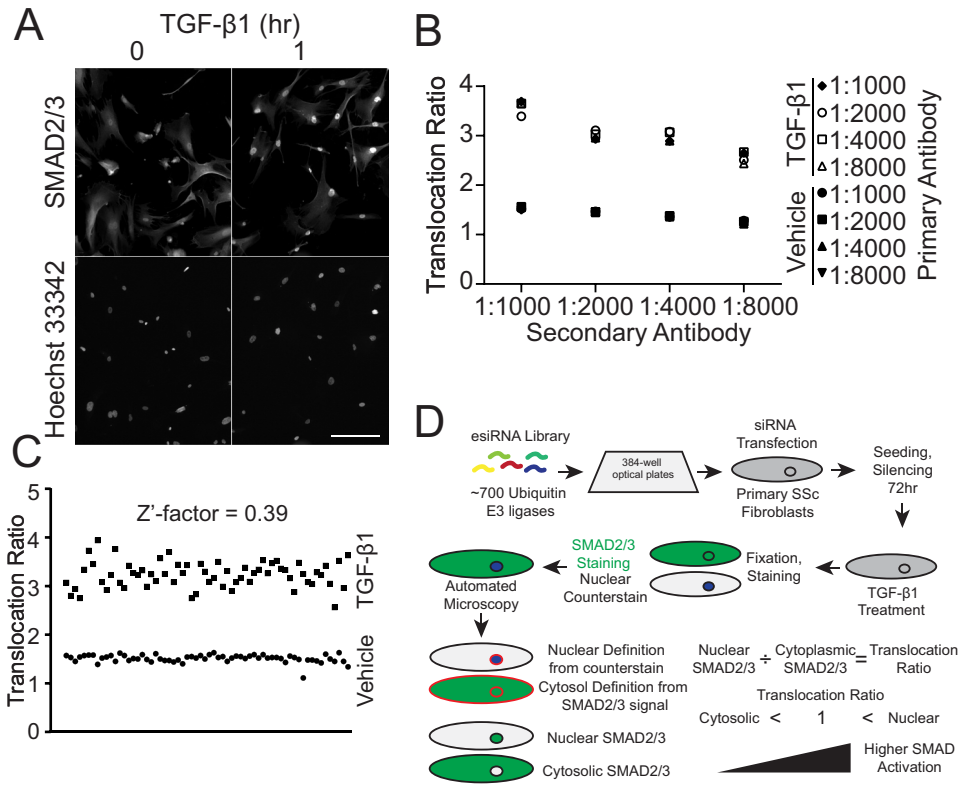

Figure 1. Assay development for scleroderma lung fibroblasts. *A*, immunofluorescence analysis of SSc lung fibroblasts for SMAD2/3 localization without and with short-term TGF-β1 stimulation. *B*, optimization of assay conditions. Translocation ratios were calculated for titrations of primary and secondary antibody without and with TGF-β1 treatment. *C*, Z′ factor calculation of the SMAD2/3 translocation ratio with vehicle or TGF-β1 treatment (n = 64 wells/treatment). *D*, Schematic of the high-content screening assay to measure SMAD translocation upon treatment with ubiqutination RNAi library. SSc cells were treated with the siRNA library in 384-well glass plates prior to TGF-β1 treatment, fixation, and staining for SMAD2/3 and the nucleus. The nucleus was segmented based on nuclear counterstain signal, and the cytosolic region was defined through expansion of the nuclear segment to the threshold of the SMAD2/3 fluorescent signal. The translocation ratio was defined as the ratio of nuclear to cytosolic signal, with a higher signal suggestive of greater SMAD activation. Translocation ratios were calculated with Gen5 software (BioTek) or CellProfiler (49). *Scale bar* = 200 μm.

ducted unbiased ubiquitin proteomics MS. We utilized LifeSensors tandem ubiquitin-binding entities (TUBE) technology to purify ubiquitinated proteins from control or *KLHL42* siRNA–treated SSc fibroblasts prior to MS (32, 33) (Fig. 3*A*). This technology uses multiple ubiquitin-binding moieties linked to resin to affinity-purify polyubiquitinated proteins from the lysate. Our hypothesis was that the putative KLHL42 substrate protein would be less ubiquitinated in *KLHL42* siRNA–treated cells (KLHL42-depleted) relative to the control. Less ubiquitinated substrate would prevent its precipitation with the TUBE pulldown; thus, the candidate substrate would be less represented in the proteomics study. The study detected 2486 total proteins, among which 155 were detected to be directly ubiquitinated (Fig. 3*B*). Among the detected proteins, 291 unique proteins were detected in solely the *KLHL42* knockdown, 464 were found only in the control sample, and 1731 were found in both samples (Fig. 3*C*). We focused our analysis on proteins disproportionately detected in the control siRNA treatment relative to *KLHL42* siRNA (464 proteins), as these proteins may have been less ubiquitinated when *KLHL42* was silenced.

We analyzed the subset of interest for any Gene Ontology terms that would be enriched relative to the total dataset using the Gene Ontology enrichment analysis and visualization tool (34). We observed that several ontology terms were significantly enriched in the control siRNA treatment group relative to the total dataset (Fig. 3*D*), including protein phosphorylation. This suggests that proteins disproportionately represented in the control siRNA group (and potential KLHL42 substrates) may be involved in protein phosphorylation. Next we investigated the set of proteins detected to be directly ubiquitinated and only found in the control siRNA treatment group for their relevance to the enriched gene ontologies (49 proteins). Of these proteins, protein phosphatase 2A regulatory subunit ϵ (PPP2R5ϵ) was one of the proteins to be detected as directly ubiquitinated and related to the process of protein phosphorylation. PPP2R5ϵ functions as a regulatory subunit for protein phosphatase 2A (PP2A) (35, 36). Intriguingly, PP2A has been implicated in regulation of fibrotic and TGF-β signaling, including SSc patient samples, suggesting that PPP2R5e might function through this pathway in SSc and be a candidate substrate of KLHL42 (37–39).

Detected PPP2R5ϵ ubiquitination on Lys-84 controls protein stability

The ubiquitin proteomics assay on SSc fibroblasts detected that PPP2R5ϵ was directly ubiquitinated, with the highest probability on Lys-84 (Fig. 4*A*). Given the proximity of two other lysine residues to Lys-84, (Lys-86 and Lys-89), there was a chance that the detected ubiquitination was on these Lys sites instead of Lys-84. Initial data analysis used a minimum local-

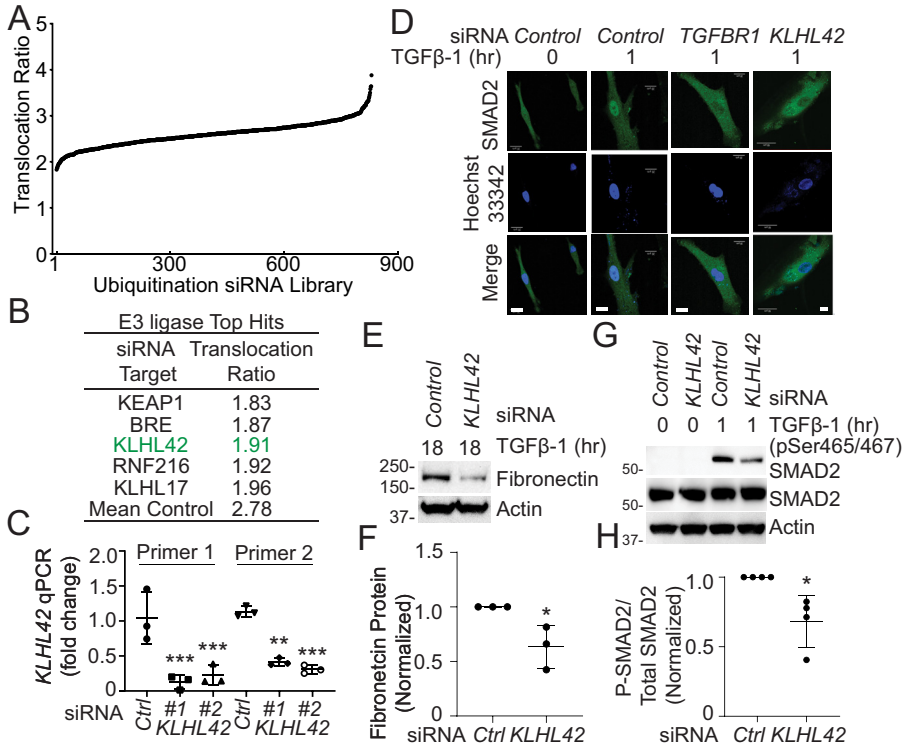

Figure 2. Depletion of ubiquitin E3 ligase KLHL42 impairs TGF-β1–mediated fibrotic signaling. *A*, screening of SSc fibroblasts with an esiRNA library targeted against ubiquitination proteins and E3 ligases by their effect on the SMAD2/3 translocation ratio. *B*, KLHL42 is a top hit from the SSc fibroblast translocation ratio screen. *C*, quantitative PCR analysis of KLHL42 knockdown by RNAi in SSc cells. Data are means ± S.D. of three independent experiments. *Ctrl*, control. *D*, knockdown of *KLHL42* impairs SMAD2 nuclear translocation upon TGF-β1 treatment. *E*, immunoblot analysis of fibrotic products following *KLHL42* knockdown and prolonged TGF-β1 treatment. *F*, quantification of the fibronectin signal from *D*. Data are means ± S.D. of three independent experiments. *G*, immunoblot analysis of SMAD2 activation following *KLHL42* knockdown and TGF-β1 treatment. *H*, quantification of phosphorylated SMAD2 (Ser-465/467) to the total SMAD2 signal from *F*. Data are means ± S.D. of four independent experiments. *, $p < 0.05$; **, $p < 0.01$; ***, $p < 0.001$ relative to controls or as indicated by one-way analysis of variance with Tukey's multiple comparisons test (*C*) or two-tailed Student's *t* test (*F* and *H*). *Scale bars* = 20 μm.

ization probability of 0.75 to remove ambiguous sites. Previous proteomic studies have detected PPP2R5ϵ to be ubiquitinated, with several other lysines corroborated by multiple studies (Lys-41, Lys-346, Lys-449, and Lys-456) (40) (Fig. 4*B*). To validate PPP2R5ϵ as a ubiquitinated substrate from the proteomics assay and to understand the ubiquitination mechanism on PPP2R5ϵ, we constructed Lys-to-Arg point mutants corresponding to detected ubiquitin conjugation sites and the results of our analysis (Lys-84, Lys-86, and Lys-89). These constructs were expressed in cells and subjected to cycloheximide (CHX) chases to assay PPP2R5ϵ protein stability (Fig. 4, *C* and *D*). We observed WT PPP2R5ϵ showed instability by 8 h of treatment, as did other lysine→arginine mutants, except for K84R. The persistence of this mutant suggests that Lys-84 is a critical ubiquitination site for PPP2R5ϵ stability.

KLHL42 facilitates PPP2R5ϵ polyubiquitination and degradation

Finally, to validate PPP2R5ϵ as a *bona fide* substrate of KLHL42, we investigated the mechanism of ubiquitination. Endogenous PPP2R5ϵ immunoprecipitated from KLHL42 siRNA–treated SSc fibroblasts showed less ubiquitination relative to the control (Fig. 5*A*). As an orthogonal approach, we ectopically expressed KLHL42-HA with His-tagged PPP2R5ϵ prior to His pulldown and ubiquitin blotting. We observed that KLHL42 coexpression enhanced the polyubiquitin signal detected upon PPP2R5ϵ precipitation (Fig. 5*B*). As substrate polyubiquitination often signals for degradation, we probed whether KLHL42 depletion affected PPP2R5ϵ protein levels and observed that *KLHL42* knockdown led to a significantly increased PPP2R5ϵ signal relative to the control (Fig. 5, *C* and *D*). We utilized other airway cells, BEAS-2B, to ectopically express KLHL42 and observed a significant dose-dependent decrease in PPP2R5ϵ protein levels (Fig. 5*E*). Further, the critical lysine site PPP2R5ϵ mutant K84R proved to be resistant to coexpression with KLHL42 (Fig. 5*F*, *lane 4*), relative to WT PPP2R5ϵ (Fig. 5*F*, *lane 2*), suggesting that KLHL42 mediates the protein stability of PPP2R5ϵ through Lys-84. These data suggest that KLHL42 regulates PPP2R5ϵ ubiquitination and protein stability. Finally, we investigated the role of PPP2R5ϵ on fibrotic signaling in SSc cells (Fig. 5, *G–I*). We observed significantly decreased PPP2R5ϵ protein upon siRNA treatment (Fig. 5, *G* and *H*). PPP2R5ϵ KD resulted in increased fibrotic production upon TGF-β1 treatment, as measured by fibronectin protein relative to control siRNA (Fig. 5, *G* and *I*). These data suggest a role of the KLHL42–PPP2R5ϵ degradation axis in fibrotic SSc signaling, as KLHL42 functions as a profibrotic mediator degrading the PP2A-enhacing subunit PPP2R5ϵ, resulting in increased fibrotic signaling (Fig. 5*J*).

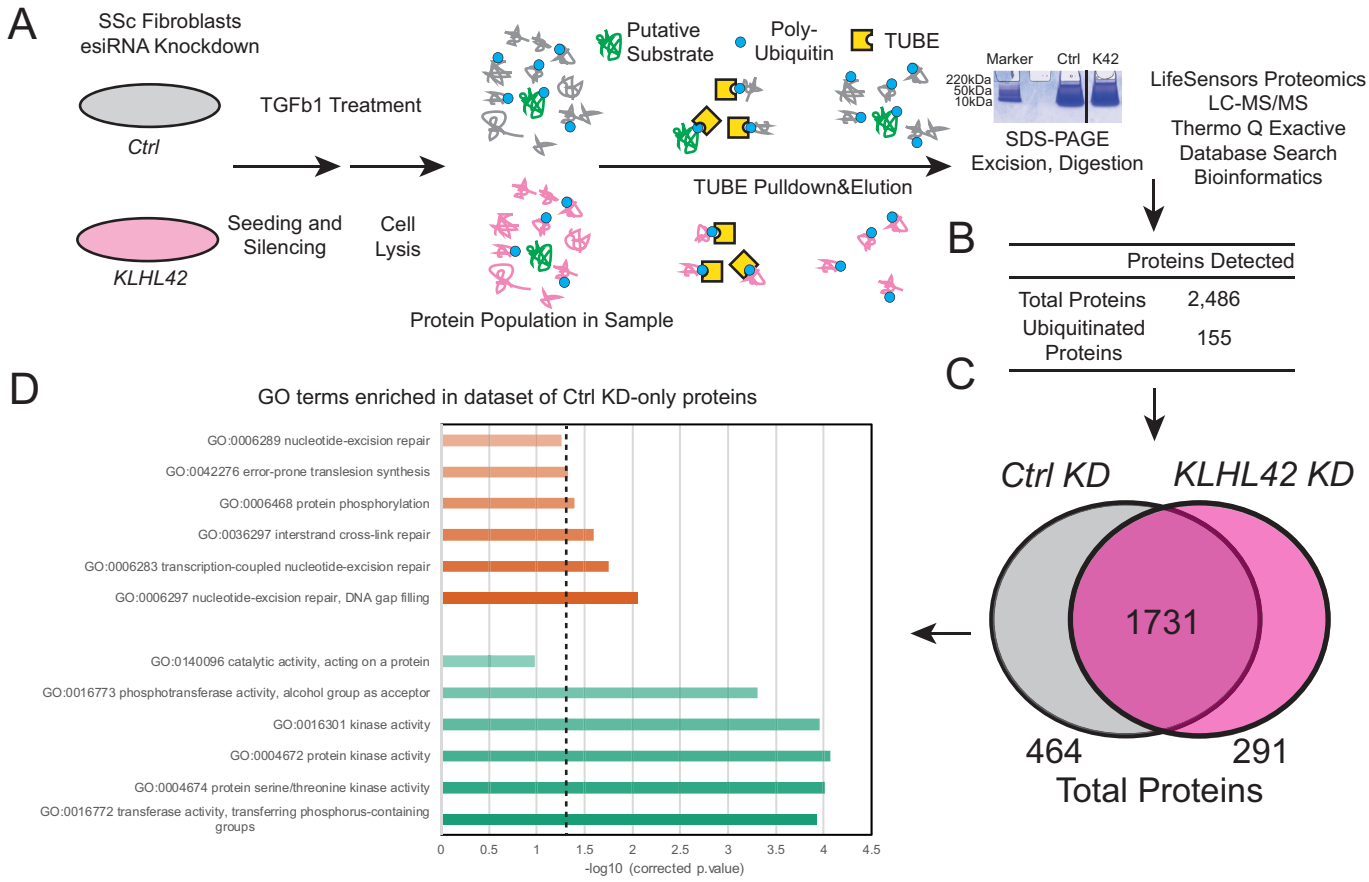

Figure 3. The ubiquitin proteomics screen uncovers PPP2R5ϵ as a potential KLHL42 substrate. *A*, schematic of the ubiquitin proteomics experiment to find KLHL42 substrates. SSc cells were treated with control (*Ctrl*) or *KLHL42* siRNA and with TGF-β1 prior to lysis and precipitation of ubiquitinated proteins with TUBE technology. Precipitated proteins were then subjected to MS analysis. *B*, total proteins detected from ubiquitin proteomics. 155 unique proteins were detected to be directly ubiquitinated. *C*, overlap of unique proteins detected between control and *KLHL42* siRNA treatments. Proteins in the control KD-only set were considered potential substrates of KLHL42. *D*, proteins detected in the control KD-only set were queried for significantly enriched Gene Ontology (*GO*) terms relative to the total dataset; several phosphorylation-related terms were significantly enriched. PPP2R5ϵ was detected in the control KD-only set and directly detected to be ubiquitinated and is a candidate substrate of KLHL42.

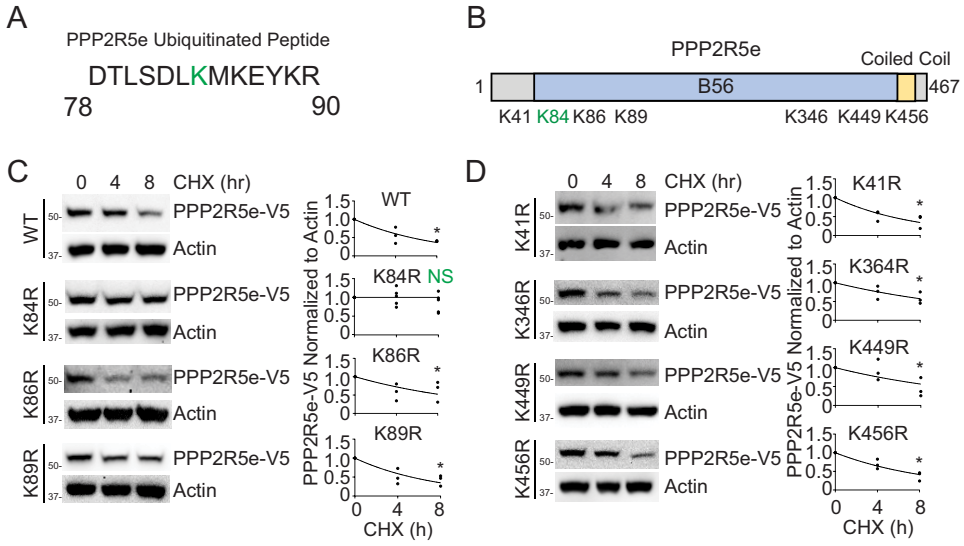

Figure 4. Lys-84 is a candidate ubiquitin acceptor site within PPP2R5ϵ. *A*, the PPP2R5ϵ peptide identified by ubiquitin proteomics spectrometry, with a high probability of a ubiquitin remnant on Lys-84. *B*, schematic of detected ubiquitin modifications of PPP2R5ϵ from the posttranslational modifications database (Phosphosite). Potentially modified lysine sites from this study (Lys-84, Lys-86, and Lys-89) are included. *C*, immunoblot analysis of PPP2R5ϵ-V5 protein and Lys-Arg mutants of suspected Lys sites from this study following a CHX time course. Data are from three to five independent experiments. *D*, immunoblot analysis of PPP2R5ϵ-V5 protein and Lys-Arg mutants of Lys sites from other studies following a CHX time course. Data are from three independent experiments. *, $p < 0.05$; *NS*, not significant ($p > 0.05$) by F test comparisons of nonlinear regression (one-phase decay), with the null hypothesis that the rate constant $k = 0$ (*C* and *D*).

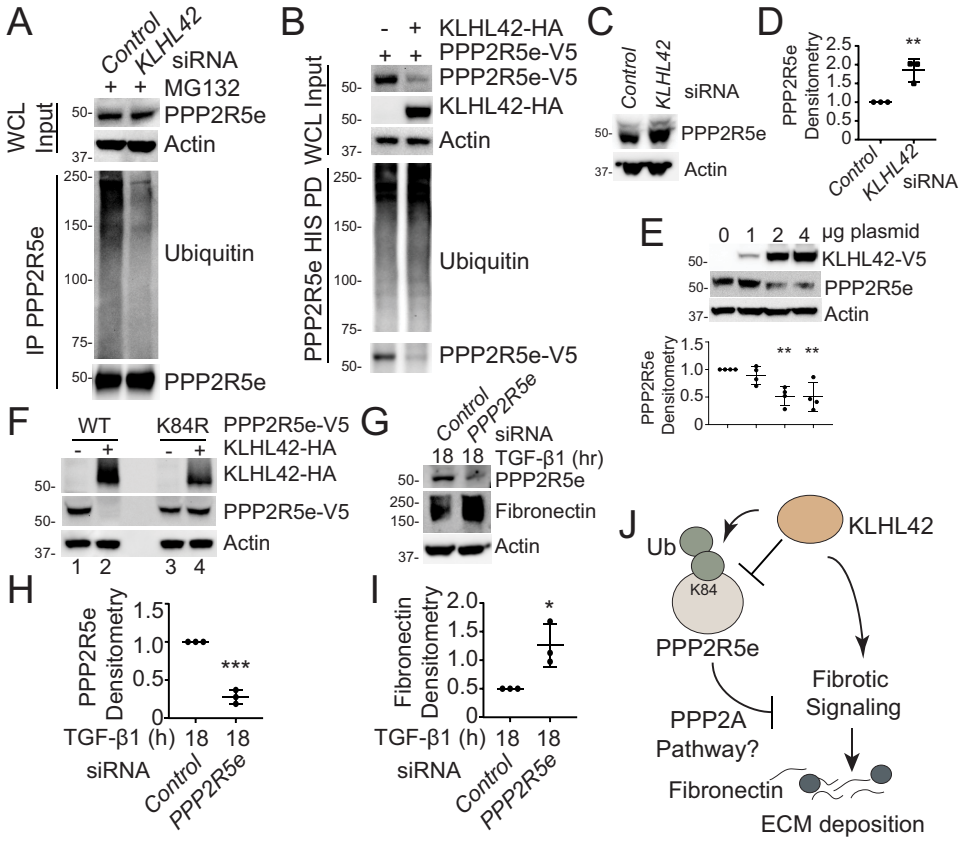

Figure 5. PPP2R5ϵ is a KLHL42 substrate and affects TGF-β signaling in SSc. *A*, immunoblot validation of the ubiquitin proteomics assay. PPP2R5ϵ protein was immunoprecipitated (*IP*) from SSc cells with control or *KLHL42* siRNA treatments. *WCL*, whole-cell lysate. *B*, immunoblot analysis of the *in vivo* ubiquitination assay in SSc cells, as PPP2R5ϵ-V5-His protein pulldown was subjected to ubiquitin immunoblotting. *C*, immunoblot analysis of PPP2R5ϵ protein level following control or *KLHL42* siRNA treatments. *D*, densitometry of *C*. Data are means ± S.D. of three independent experiments. *E*, immunoblot analysis of PPP2R5ϵ protein following dose overexpression of the KLHL42-V5 plasmid. Data are means ± S.D. of four independent experiments. *F*, WT or K84R mutant PPP2R5ϵ-V5 was expressed without or with coexpression of KLHL42-HA prior to blotting. *G*, SSc cells were treated with *PPP2R5ϵ* siRNA prior to 18-h TGF-β1 treatment and immunoblotting. *H* and *I*, densitometry of PPP2R5ϵ (*H*) and fibronectin (*I*) protein without and with *PPP2R5ϵ* knockdown and 18-h TGF-β1 treatment. Data are means ± S.D. of three independent experiments. *J*, schematic of the proposed model, in which KLHL42 controls the ubiquitination (*Ub*) and stability of PPP2R5ϵ. PPP2R5ϵ affects PP2A antifibrotic activity and downstream fibrotic signaling, leading KLHL42 to be a profibrotic regulator in SSc. *, $p < 0.05$; ***, $p < 0.001$; two-tailed Student's *t* test (*D*, *H*, and *I*). **, $p < 0.01$ by analysis of variance with Dunnett's multiple comparisons test (*E*).

Discussion

This study demonstrated SMAD2/3 immunostaining and automated microscopy as a screening tool for SSc cells. We calculated a translocation ratio of the SMAD signal as a surrogate for TGF-β pathway activity. This assay system is robust and shows good assay parameters with a Z-factor of 0.39. We observed that knockdown of the E3 ligase KLHL42 acutely affects SMAD localization and affects downstream TGF-β/fibrotic signaling, suggesting that KLHL42 is a profibrotic E3 ligase. To uncover potential KLHL42 substrates, we conducted unbiased MS ubiquitin proteomics. Through bioinformatic analysis, PPP2R5ϵ emerged as a putative substrate, and we confirmed Lys-84 as a critical site for PPP2R5ϵ stability through an unbiased proteomics and mutagenesis assay. Finally, we demonstrated that KLHL42 facilitates polyubiquitination of PPP2R5ϵ, leading to its degradation, and that knockdown of PPP2R5ϵ increases fibrotic protein production, potentially through the PP2A pathway.

Phosphatase control of TGF-β signaling is a major mechanism in SSc. PP2A has been shown to play a direct role in regulating fibrotic signaling in primary SSc disease models. TGF-β treatment was observed to affect PP2A modulation of ERK1/2 activation in SSc fibroblast autocrine signaling (41). extracellular signal-regulated kinase activation has been directly implicated in dysfunction mechanics from SSc fibroblasts and has been observed to be constitutively activated in fibroblasts (42, 43). Further, TGF-β treatment of dermal fibroblasts causes a decrease in PP2A transcript/protein levels (38). The regulatory subunit PPP2R5ϵ belongs to the B56/B' family and modulates overall PP2A activity (35). PPP2R5ϵ expression leads directly to more dephosphorylation of PP2A substrates, suggesting that PPP2R5ϵ is an enhancer of PP2a activity (36). This is in line with our functional observations, as we observed that PPP2R5ϵ knockdown led to increased fibrotic signaling. Most research has emphasized the role of PPP2R5ϵ in neoplasia; this is the first study to suggest a function in SSc-ILD fibrotic signaling. More studies are needed to characterize the exact molecular mechanisms of KLHL42 control of PPP2R5ϵ and PP2A signaling.

E3 ligases may play an important role in SSc-ILD signaling. Our previous studies have shown that E3 ligases can potently control fibrotic signaling through targeted degradation of key signal transduction (24). There is evidence that this paradigm

can be extended to SSc-ILD fibrotic signaling as well (44, 45). Further, therapeutic targeting of ubiquitination may show promise for lung fibrotic diseases. Recent studies have shown that inhibition of the E3 ligase Skp2 ameliorates fibrotic phenotypes in mice (46), and pharmacological inactivation of Cullin-type E3 ligases is protective in experimental pulmonary fibrosis models (21). Current therapeutic options in SSc-ILD are limited, and ubiquitin E3 ligases may prove to be new targets for intervention. In conclusion, we utilized two unbiased approaches (siRNA screen and proteomics) to discover the ubiquitin E3 ligase KLHL42 as a mediator of fibrotic signaling in SSc-ILD through regulation of PPP2R5ϵ ubiquitination and stability.

Experimental procedures

Materials

PPP2R5ϵ complementary DNA was from DNASU (HsCD00735088) (47). The QuikChange II XL site-directed mutagenesis kit (200521) was from Agilent. BEAS-2B cells (CRL-9609) were from the ATCC. The anti-HA tag (6E2, 2367S), anti-ubiquitin (P4D1, 3936), anti-phospho-Smad2 (Ser-465/467, 138D4, 3108), and anti-Smad2/3 (D7G7, 8685) were from Cell Signaling Technology. 384-well glass-bottom tissue culture plates (P384-1.5H-N) were from Cellvis. The antibiotic–antimycotic supplement (15240062), DMEM (10569044), DMEM-F12 (11330057), FBS (26140079), and penicillin–streptomycin (15140122) were from Gibco. Lullaby siRNA transfection reagent (LL7) was from OzBiosciences. hTGF-β1 (100-21) was from PeproTech. Anti-PPP2R5e (NBP1-79638) was from Novus. Anti-fibronectin (EP5, sc-8422) and anti-PPP2R5ϵ (A-11, sc-376176) were from Santa Cruz Biotechnology. His tag Dynabeads (10103D) and Hoechst 33342 (H3570) were from Invitrogen. Anti-β-actin (AC-15, A5441) was from Sigma-Aldrich. Anti-rabbit IgG, Alexa Fluor 488 (A-11008), the anti-V5 tag (R960), protein A/G magnetic beads (88802), and the pcDNA3.1D TOPO kit (K490001) were from Thermo Fisher. Primers for cloning and Dicer-Substrate Short Interfering RNAs were from IDT. The custom siRNA library was from Sigma-Aldrich. Anti-mouse IgG HRP (18-8817-30) and anti-rabbit IgG HRP (18-8816-31) were from Rockland Immunochemicals. MG-132 (F1101) was from UBP BIO. Cytation5 was from BioTek.

Cell culture

Primary SSc patient lung fibroblasts were cultured in DMEM (Gibco) according to a previous technique (27, 48). BEAS-2b cells were cultured in HITES (DMEM-F12 (Gibco), Sodium selenite 38 nM, Insulin 0.01 mg/ml, Transferrin 0.005 mg/ml, HEPES 10 mM, L-glutamine 2 mM medium supplemented with 10% FBS. Cells were treated with cycloheximide (100 μg/ml) and transfected with Nucleofector 2b (Amaxa), XtremeGene HP plasmid reagent (Roche), XtremeGene siRNA reagent (Roche), or Lullaby siRNA reagent (OzBiosciences). TGF-β1 (PeproTech) was treated at 2 ng/ml for the indicated times in DMEM without FBS supplementation.

siRNA transfection

Cells were seeded to a confluency of 50% before siRNA transfection. siRNA was transfected using Lullaby siRNA reagent (OzBiosciences). 1 μg of siRNA was mixed with 10 μl of Lullaby reagent in 1/10th of the final cell volume for 25 min and added dropwise to cells. Knockdown proceeded for 48–72 h prior to cell collection and analysis. Sequences of dsiRNA used were as follows: KLHL42 siRNA 1, 5′rCrUrUrArUrCrArGrUrGrUrCrCrUrUrGrArCrArArGrCrATT3′ and 5′rArArUrGrCrUrUrGrUrCrArArGrGrArCrArCrUrGrArUrArArGrGrArA3; KLHL42 siRNA 2, 5′rArCrUrCrUrGrArArArUrUrArUrCrUrGrArUrArUrUrUrUGT-3′ and 5′rArCrArArArArUrArUrUrCrArGrArUrArArUrUrUrCrArGrArGrUrGrU-3′; PPP2R5ϵ siRNA, 5′rCrArGrCrUrArArUrUrArUrGrGrArUrArUrUrGrUrCrArUCT-3′ and 5′rArGrArUrGrArCrArArUrArUrCrCrArUrArArUrUrArArGrCrUrGrArC-3′; TGF-βR1 siRNA, 5′rGrUrUrUrGrArArUrArUrUrCrUrCrArCrArUrCrArArGrCTT-3′ and 5′rArArGrCrUrUrGrArUrGrUrGrArGrArArUrArUrUrCrArArArCrArU-3′.

Immunoprecipitation and immunoblotting

Cells were lysed in immunoprecipitation buffer (50 mM Tris-HCl (pH 7.6), 150 mM NaCl, and 0.25% v/v Triton X-100) and centrifuged at 10,000 × g for 10 min at 4 °C. The supernatant was incubated for 2 h at 4 °C with 1:100 dilution of immunoprecipitating antibody. The antibody was captured with protein A/G beads (Thermo Fisher) for an additional 2 h. The immunoprecipitate was washed three times with immunoprecipitation buffer and eluted in 1× Laemmli buffer at 88 °C for 5 min prior to immunoblot analysis. Immunoprecipitated samples were blotted with anti-mouse or anti-rabbit TrueBlot (Rockland).

Cloning

Recombinant DNA constructs were prepared through PCR cloning techniques and cloned into the pcDNA3.1D vector (Thermo Fisher) unless otherwise noted. Point mutants were generated with the QuikChange XL 2 site-directed mutagenesis kit (Agilent). All constructs were validated by DNA sequencing (Genewiz).

Ubiquitination siRNA SMAD translocation screen

Primary SSc patient lung fibroblast cells were seeded in 384-well glass-bottom plates (Cellvis, 5000 cells/well) and transfected with Mission esiRNA-targeting ubiquitination proteins (E1, E2, E3 ligases etc.) (Sigma-Aldrich) using XtremeGene siRNA transfection reagent (Roche). Knockdown proceeded for 72 h prior to TGF-β1 (Peprotech, 2 ng/ml) stimulation for 1 h. Cells were then fixed (4% paraformaldehyde), permeabilized (0.5% Triton X-100), and stained for endogenous SMAD2/3 (Cell Signaling Technology), followed by goat anti-rabbit Alexa Fluor 488 or 647 (Invitrogen) and nuclear counterstain with Hoechst 33342 (Invitrogen). The fluorescent signal was imaged using Cytation5 (BioTek) or Image Express (Molecular Devices). The SMAD2/3 translocation ratio (nuclear to cytosolic signal) was calculated and analyzed by CellProfiler (49) or Gen5 software (BioTek).

Ubiquitin proteomics

Ubiquitin proteomics and TUBE experiments were conducted at LifeSensors. Experimental and control samples were

analyzed using biological duplicates. Use of biological replicates allowed better accounting for variability with each step of the MS workflow (cell culture, sample preparation, and analysis).

Samples were spun down, and duplicate 22-μl volumes of each sample were mixed with SDS loading buffer. Samples were heated at 90 °C for 5 min and run on SDS-PAGE prior to Coomassie Blue staining. The remaining sample was run on a different gel, resulting in each sample being run on a total of three gel lanes. The lanes were excised, reduced with tris(2-carboxyethyl)phosphine, alkylated with iodoacetamide, and digested with trypsin. Tryptic digests were analyzed using a 150-min LC run on a Thermo Q Exactive HF mass spectrometer. A 30-min blank was run between samples.

Ubiquitin proteomics resulted in four RAW files, two each for KLHL42 siRNA treatment and control siRNA treatment. MaxQuant 1.6.2.3 was used to query MS data against the Uniprot human database (2018_10_01); 196,371 entries were specifically searched. The first search peptide mass tolerance was set at 20 ppm; the main search peptide tolerance was set at 4.5 ppm. Fragment ion mass tolerance was set at 20 ppm. The protein, peptide, and site false discovery rate was set at 1%. Full trypsin specificity was used to generate peptides, with a maximum of three missed cleavages permitted. Carabimidomethyl (C) was set as a fixed modification, with acetyl (protein N-term), oxidation (M), and GlyGly (K) considered variable modifications.

Protein quantification was performed using Razor and unique peptides. Razor peptides are shared (nonunique) peptides assigned to the protein group with the most other peptides (Occam's razor principle). Quantitation was based on the sum of the peptide MS peak areas for the protein (intensity) because of its increased accuracy compared with the MS/MS count. To account for the fact that larger proteins generate more peptides, the intensity values were adjusted by normalizing against the number of theoretical peptides for each protein (Intensity Based Absolute Quantification (iBAQ) intensity). We then sorted (largest to smallest order) on the iBAQ values to determine which proteins were more abundant in a sample. Data were then analyzed via the Gene Ontology enrichment analysis and visualization tool, querying the 464 proteins identified solely in the control siRNA treatments (and that may have lost ubiquitination when KLHL42 was knocked down) for their gene ontologies as described previously (34). The sets of proteins detected to be directly ubiquitinated and only found in the control siRNA treatment group (49 proteins) were inspected manually based on their relevance to the enriched gene ontologies, leading to the uncovering of PPP2R5ϵ.

Confocal microscopy

SSc cells were seeded in 35-mm MatTek glass-bottom dishes before siRNA knockdown and TGF-β1 treatment. Cells were washed with 1× PBS prior to fixation with 4% paraformaldehyde and permeabilization with 0.5% Triton X-100. Following blocking with 2% BSA in PBS, cells were exposed to SMAD2 primary antibody (1:500) overnight and then 1:1000 Alexa Fluor 488 secondary antibodies for immunostaining. The nucleus was counterstained with Hoechst 33342. Cells were visualized with a Nikon A1 confocal microscope using 405-, 488-, or 567-nm wavelengths. All experiments were done with a ×60 oil differential interference contrast objective lens.

Statistics

All statistical tests were calculating using GraphPad Prism 8. $p < 0.05$ was used to indicate significance. Densitometry was calculated using ImageJ (National Institutes of Health).

Data availability

Ubiquitin proteomics data have been uploaded through the MassIVE repository, ID: MSV000084800. The MSViewer Data can be accessed using the key axtpvumdao.

Author contributions—T. B. L., D. J. K., J. W. E., R. L., Y. L., and B. B. C. conceptualization; T. B. L., M. B. L., J. R. K., and E.V. data curation; T. B. L., M. B. L., J. R. K., C. M., and Y. L. formal analysis; T. B. L., M. J. J., D. J. K., J. W. E., R. L., Y. L., and B. B. C. funding acquisition; T. B. L., K. C. L., M. B. L., F. T., C. M., D. J. K., J. W. E., R. L., Y. L., and B. B. C. investigation; T. B. L., K. C. L., M. B. L., F. T., J. R. K., Y. L., and B. B. C. visualization; T. B. L., M. B. L., F. T., J. R. K., E. V., T. T., D. J. K., J. W. E., R. L., Y. L., and B. B. C. methodology; T. B. L., Y. L., and B. B. C. writing-original draft; T. B. L., C. M., E. V., T. T., M. J. J., D. J. K., J. W. E., R. L., Y. L., and B. B. C. project administration; T. B. L., D. J. K., J. W. E., T.F., R. L., Y. L., and B. B. C. writing-review and editing; M. B. L., J. R. K., C. M., E. V., T. T., J. W. E., R. L., and Y. L. software; M. B. L., F. T., J. R. K., R. L., and Y. L. validation; C. M., E. V., T. T., D. J. K., J. W. E., T. F., R. L., Y. L., and B. B. C. resources; D. J. K., J. W. E., T. F., R. L., Y. L., and B. B. C. supervision.

Acknowledgments—We thank the University of Pittsburgh Medical Center lung transplantation team for procurement of the lungs, the Center for Organ Recovery and Education, and the organ donors and their families for generous donation of the tissues used in this study.

References

1. Denton, C. P., and Khanna, D. (2017) Systemic sclerosis. *Lancet* **390,** 1685–1699 CrossRef Medline
2. Poudel, D. R., Jayakumar, D., Danve, A., Sehra, S. T., and Derk, C. T. (2018) Determinants of mortality in systemic sclerosis: a focused review. *Rheumatol. Int.* **38,** 1847–1858 CrossRef Medline
3. Barnes, J., and Mayes, M. D. (2012) Epidemiology of systemic sclerosis: incidence, prevalence, survival, risk factors, malignancy, and environmental triggers. *Curr. Opin. Rheumatol.* **24,** 165–170 CrossRef Medline
4. Denton, C. P., Wells, A. U., and Coghlan, J. G. (2018) Major lung complications of systemic sclerosis. *Nat. Rev. Rheumatol.* **14,** 511–527 CrossRef Medline
5. Korman, B. (2019) Evolving insights into the cellular and molecular pathogenesis of fibrosis in systemic sclerosis. *Transl. Res.* **209,** 77–89 CrossRef Medline
6. Giacomelli, R., Liakouli, V., Berardicurti, O., Ruscitti, P., Di Benedetto, P., Carubbi, F., Guggino, G., Di Bartolomeo, S., Ciccia, F., Triolo, G., and Cipriani, P. (2017) Interstitial lung disease in systemic sclerosis: current and future treatment. *Rheumatol. Int.* **37,** 853–863 CrossRef Medline
7. Lafyatis, R. (2014) Transforming growth factor β: at the centre of systemic sclerosis. *Nat. Rev. Rheumatol.* **10,** 706–719 CrossRef Medline
8. Shi, Y., and Massagué, J. (2003) Mechanisms of TGF-β signaling from cell membrane to the nucleus. *Cell* **113,** 685–700 CrossRef Medline
9. Massagué, J. (2012) TGFβ signalling in context. *Nat. Rev. Mol. Cell Biol.* **13,** 616–630 CrossRef Medline

10. Imoto, S., Sugiyama, K., Muromoto, R., Sato, N., Yamamoto, T., and Matsuda, T. (2003) Regulation of transforming growth factor-β signaling by protein inhibitor of activated STAT, PIASy through Smad3. *J. Biol. Chem.* **278,** 34253–34258 CrossRef Medline
11. Lee, P. S., Chang, C., Liu, D., and Derynck, R. (2003) Sumoylation of Smad4, the common Smad mediator of transforming growth factor-β family signaling. *J. Biol. Chem.* **278,** 27853–27863 CrossRef Medline
12. Abdollah, S., Macías-Silva, M., Tsukazaki, T., Hayashi, H., Attisano, L., and Wrana, J. L. (1997) TβRI phosphorylation of Smad2 on Ser465 and Ser467 is required for Smad2-Smad4 complex formation and signaling. *J. Biol. Chem.* **272,** 27678–27685 CrossRef Medline
13. Macías-Silva, M., Abdollah, S., Hoodless, P. A., Pirone, R., Attisano, L., and Wrana, J. L. (1996) MADR2 is a substrate of the TGFβ receptor and its phosphorylation is required for nuclear accumulation and signaling. *Cell* **87,** 1215–1224 CrossRef Medline
14. Derynck, R., and Zhang, Y. E. (2003) Smad-dependent and Smad-independent pathways in TGF-β family signalling. *Nature* **425,** 577–584 CrossRef Medline
15. Inoue, Y., and Imamura, T. (2008) Regulation of TGF-β family signaling by E3 ubiquitin ligases. *Cancer Sci.* **99,** 2107–2112 CrossRef Medline
16. Izzi, L., and Attisano, L. (2004) Regulation of the TGFβ signalling pathway by ubiquitin-mediated degradation. *Oncogene* **23,** 2071–2078 CrossRef Medline
17. Varshavsky, A. (2017) The ubiquitin system, autophagy, and regulated protein degradation. *Annu. Rev. Biochem.* **86,** 123–128 CrossRef Medline
18. Gao, S., Alarcón, C., Sapkota, G., Rahman, S., Chen, P.-Y., Goerner, N., Macias, M. J., Erdjument-Bromage, H., Tempst, P., and Massagué, J. (2009) Ubiquitin ligase Nedd4L targets activated Smad2/3 to limit TGF-β signaling. *Mol. Cell* **36,** 457–468 CrossRef Medline
19. Kavsak, P., Rasmussen, R. K., Causing, C. G., Bonni, S., Zhu, H., Thomsen, G. H., and Wrana, J. L. (2000) Smad7 binds to Smurf2 to form an E3 ubiquitin ligase that targets the TGFβ receptor for degradation. *Mol. Cell* **6,** 1365–1375 CrossRef Medline
20. Li, S., Zhao, J., Shang, D., Kass, D. J., and Zhao, Y. (2018) Ubiquitination and deubiquitination emerge as players in idiopathic pulmonary fibrosis pathogenesis and treatment. *JCI Insight* **3,** CrossRef Medline
21. Deng, Q., Zhang, J., Gao, Y., She, X., Wang, Y., Wang, Y., and Ge, X. (2017) MLN4924 protects against bleomycin-induced pulmonary fibrosis by inhibiting the early inflammatory process. *Am. J. Transl. Res.* **9,** 1810–1821 Medline
22. Collison, A. M., Li, J., de Siqueira, A. P., Lv, X., Toop, H. D., Morris, J. C., Starkey, M. R., Hansbro, P. M., Zhang, J., and Mattes, J. (2019) TRAIL signals through the ubiquitin ligase MID1 to promote pulmonary fibrosis. *BMC Pulm. Med.* **19,** 31 CrossRef Medline
23. Zuscik, M. J., Rosier, R. N., and Schwarz, E. M. (2003) Altered negative regulation of transforming growth factor β signaling in scleroderma: potential involvement of SMURF2 in disease. *Arthritis Rheum.* **48,** 1779–1780 CrossRef Medline
24. Lear, T., McKelvey, A. C., Rajbhandari, S., Dunn, S. R., Coon, T. A., Connelly, W., Zhao, J. Y., Kass, D. J., Zhang, Y., Liu, Y., and Chen, B. B. (2016) Ubiquitin E3 ligase FIEL1 regulates fibrotic lung injury through SUMO-E3 ligase PIAS4. *J. Exp. Med.* **213,** 1029–1046 CrossRef Medline
25. Lear, T., and Chen, B. B. (2016) Therapeutic targets in fibrotic pathways. *Cytokine* **88,** 193–195 CrossRef Medline
26. Liu, S.-S., Lv, X.-X., Liu, C., Qi, J., Li, Y.-X., Wei, X.-P., Li, K., Hua, F., Cui, B., Zhang, X.-W., Yu, J.-J., Yu, J.-M., Wang, F., Shang, S., Zhao, C.-X., *et al.* (2019) Targeting degradation of the transcription factor C/EBPβ reduces lung fibrosis by restoring activity of the ubiquitin-editing enzyme A20 in macrophages. *Immunity* **51,** 522–534.e7 CrossRef Medline
27. Valenzi, E., Bulik, M., Tabib, T., Morse, C., Sembrat, J., Trejo Bittar, H., Rojas, M., and Lafyatis, R. (2019) Single-cell analysis reveals fibroblast heterogeneity and myofibroblasts in systemic sclerosis-associated interstitial lung disease. *Ann. Rheum. Dis.* **78,** 1379–1387 CrossRef Medline
28. Mori, Y., Chen, S.-J., and Varga, J. (2003) Expression and regulation of intracellular SMAD signaling in scleroderma skin fibroblasts. *Arthritis Rheum.* **48,** 1964–1978 CrossRef Medline
29. Zhang, J. H., Chung, T. D., and Oldenburg, K. R. (1999) A simple statistical parameter for use in evaluation and validation of high throughput screening assays. *J. Biomol. Screen.* **4,** 67–73 CrossRef Medline
30. Petroski, M. D., and Deshaies, R. J. (2005) Function and regulation of cullin-RING ubiquitin ligases. *Nat. Rev. Mol. Cell Biol.* **6,** 9–20 CrossRef Medline
31. Cummings, C. M., Bentley, C. A., Perdue, S. A., Baas, P. W., and Singer, J. D. (2009) The Cul3/Klhdc5 E3 ligase regulates p60/katanin and is required for normal mitosis in mammalian cells. *J. Biol. Chem.* **284,** 11663–11675 CrossRef Medline
32. Hjerpe, R., Aillet, F., Lopitz-Otsoa, F., Lang, V., England, P., and Rodriguez, M. S. (2009) Efficient protection and isolation of ubiquitylated proteins using tandem ubiquitin-binding entities. *EMBO Rep.* **10,** 1250–1258 CrossRef Medline
33. Azkargorta, M., Escobes, I., Elortza, F., Matthiesen, R., and Rodríguez, M. S. (2016) TUBEs-mass spectrometry for identification and analysis of the ubiquitin-proteome. *Methods Mol. Biol.* **1449,** 177–192 CrossRef Medline
34. Eden, E., Navon, R., Steinfeld, I., Lipson, D., and Yakhini, Z. (2009) GOrilla: a tool for discovery and visualization of enriched GO terms in ranked gene lists. *BMC Bioinformatics* **10,** 48 CrossRef Medline
35. McCright, B., and Virshup, D. M. (1995) Identification of a new family of protein phosphatase 2A regulatory subunits. *J. Biol. Chem.* **270,** 26123–26128 CrossRef Medline
36. Cristóbal, I., Cirauqui, C., Castello-Cros, R., Garcia-Orti, L., Calasanz, M. J., and Odero, M. D. (2013) Downregulation of PPP2R5E is a common event in acute myeloid leukemia that affects the oncogenic potential of leukemic cells. *Haematologica* **98,** e103–e104 CrossRef Medline
37. Xia, H., Seeman, J., Hong, J., Hergert, P., Bodem, V., Jessurun, J., Smith, K., Nho, R., Kahm, J., Gaillard, P., and Henke, C. (2012) Low α(2)β(1) integrin function enhances the proliferation of fibroblasts from patients with idiopathic pulmonary fibrosis by activation of the β-catenin pathway. *Am. J. Pathol.* **181,** 222–233 CrossRef Medline
38. Samuel, G. H., Bujor, A. M., Nakerakanti, S. S., Hant, F. N., and Trojanowska, M. (2010) Autocrine transforming growth factor β signaling regulates extracellular signal-regulated kinase 1/2 phosphorylation via modulation of protein phosphatase 2A expression in scleroderma fibroblasts. *Fibrogenesis Tissue Repair* **3,** 25 CrossRef Medline
39. Rizvi, F., Siddiqui, R., DeFranco, A., Homar, P., Emelyanova, L., Holmuhamedov, E., Ross, G., Tajik, A. J., and Jahangir, A. (2018) Simvastatin reduces TGF-β1-induced SMAD2/3-dependent human ventricular fibroblasts differentiation: role of protein phosphatase activation. *Int. J. Cardiol.* **270,** 228–236 CrossRef Medline
40. Hornbeck, P. V., Zhang, B., Murray, B., Kornhauser, J. M., Latham, V., and Skrzypek, E. (2015) PhosphoSitePlus, 2014: mutations, PTMs and recalibrations. *Nucleic Acids Res.* **43,** D512–D520 CrossRef Medline
41. Asano, Y., Ihn, H., Yamane, K., Jinnin, M., Mimura, Y., and Tamaki, K. (2005) Increased expression of integrin α (v) β3 contributes to the establishment of autocrine TGF-β signaling in scleroderma fibroblasts. *J. Immunol.* **175,** 7708–7718 CrossRef Medline
42. Bhattacharyya, S., Chen, S.-J., Wu, M., Warner-Blankenship, M., Ning, H., Lakos, G., Mori, Y., Chang, E., Nihijima, C., Takehara, K., Feghali-Bostwick, C., and Varga, J. (2008) Smad-independent transforming growth factor-β regulation of early growth response-1 and sustained expression in fibrosis: implications for scleroderma. *Am. J. Pathol.* **173,** 1085–1099 CrossRef Medline
43. Chen, Y., Leask, A., Abraham, D. J., Pala, D., Shiwen, X., Khan, K., Liu, S., Carter, D. E., Wilcox-Adelman, S., Goetinck, P., Denton, C. P., Black, C. M., Pitsillides, A. A., Sarraf, C. E., and Eastwood, M. (2008) Heparan sulfate-dependent ERK activation contributes to the overexpression of fibrotic proteins and enhanced contraction by scleroderma fibroblasts. *Arthritis Rheum.* **58,** 577–585 CrossRef Medline
44. Meiners, S., Evankovich, J., and Mallampalli, R. K. (2018) The ubiquitin proteasome system as a potential therapeutic target for systemic sclerosis. *Transl. Res.* **198,** 17–28 CrossRef Medline
45. Long, Y., Chen, W., Du, Q., Zuo, X., and Zhu, H. (2018) Ubiquitination in scleroderma fibrosis and its treatment. *Front. Immunol.* **9,** 2383 CrossRef Medline

46. Mikamo, M., Kitagawa, K., Sakai, S., Uchida, C., Ohhata, T., Nishimoto, K., Niida, H., Suzuki, S., Nakayama, K. I., Inui, N., Suda, T., and Kitagawa, M. (2018) Inhibiting Skp2 E3 Ligase suppresses bleomycin-induced pulmonary fibrosis. *Int. J. Mol. Sci.* **19,** 474 CrossRef Medline
47. Seiler, C. Y., Park, J. G., Sharma, A., Hunter, P., Surapaneni, P., Sedillo, C., Field, J., Algar, R., Price, A., Steel, J., Throop, A., Fiacco, M., and LaBaer, J. (2014) DNASU plasmid and PSI:Biology-Materials repositories: resources to accelerate biological research. *Nucleic Acids Res.* **42,** D1253–D1260 CrossRef Medline
48. Morse, C., Tabib, T., Sembrat, J., Buschur, K. L., Bittar, H. T., Valenzi, E., Jiang, Y., Kass, D. J., Gibson, K., Chen, W., Mora, A., Benos, P. V., Rojas, M., and Lafyatis, R. (2019) Proliferating SPP1/MERTK-expressing macrophages in idiopathic pulmonary fibrosis. *Eur. Respir. J.* **54,** 1802441 CrossRef Medline
49. Carpenter, A. E., Jones, T. R., Lamprecht, M. R., Clarke, C., Kang, I. H., Friman, O., Guertin, D. A., Chang, J. H., Lindquist, R. A., Moffat, J., Golland, P., and Sabatini, D. M. (2006) CellProfiler: image analysis software for identifying and quantifying cell phenotypes. *Genome Biol.* **7,** R100 CrossRef Medline